Virtual Planning and Simulation of Coarctation Repair in Hypoplastic Aortic Arches: Is Fixing the Coarctation Alone Enough?

Seda Aslan[1], Xiaolong Liu[1], Qiyuan Wu[1], Paige Mass[2], Yue-Hin Loke[2], Narutoshi Hibino[3], Laura Olivieri[2] and Axel Krieger[1]

[1]*Department of Mechanical Engineering, Johns Hopkins University, Baltimore, MD, U.S.A.*

[2]*Division of Cardiology, Children's National Hospital, Washington DC, U.S.A.*

[3]*Section of Cardiac Surgery, Department of Surgery, The University of Chicago Medicine, Chicago, IL, U.S.A.*

Keywords: Virtual Aorta Repair, Coarctation of Aorta, Transverse Arch Hypoplasia, Computational Fluid Dynamics.

Abstract: Coarctation of aorta (CoA) is a congenital heart disease that may coexist with transverse arch hypoplasia (TAH). Infants who suffer from both conditions are often treated only for CoA at the initial repair if the degree of TAH is diagnosed as mild. In this study, we investigated the effect of virtually repairing the CoA of three patients (n=3) who also suffer from TAH. We repaired the CoA by using virtual stents that were modeled based on descending aorta diameters of the patients. Using computational fluid dynamics (CFD) simulations, we investigated the changes in time-averaged wall shear stress (TAWSS) after the virtual repair and calculated the peak systolic pressure drop (PSPD), which is the indicator of the performance of the repair. The magnitude of TAWSS was reduced in the repaired CoA regions in all the patients. The PSPD was improved in two patients, remaining above 20 mmHg in one of them. There was no significant change in PSPD for one patient after the virtual repair. The results may potentially help clinicians to gain better insights into whether the CoA repair alone in patients with existing TAH is sufficient.

1 INTRODUCTION

Coarctation of aorta (CoA) is a narrowing that usually occurs in the region distal to the left subclavian artery. It is a congenital defect that affects approximately 2200 newborns every year in the United States (Mai et al., 2019). Infantile CoA is often accompanied by transverse arch hypoplasia (TAH). Different from CoA, TAH involves a larger narrowed portion of the aorta (Ma et al., 2017). The condition of TAH can be severe and the treatment of TAH may require surgical repair. CoA and TAH are associated with upper body hypertension (Kenny et al., 2011), left ventricular dysfunction, and aortic aneurysm formation (Schubert et al., 2020). Depending on the degree of TAH, the clinicians may decide to repair only CoA when the TAH is mild (Siewers et al., 1991).

TAH repair is a very extensive procedure that is performed on bypass via a sternotomy to reconstruct the aortic arch structure by using vascular patches or grafts. Compared to TAH repair, the procedure to repair CoA alone typically has less technical complexity and does not require cardiopulmonary bypass. The common procedures to treat CoA include surgical techniques such as resection with end-to-end anastomosis and tubular bypass grafts (Liu et al., 2020; Rao, 2020), and minimally invasive catheter-based techniques such as balloon angioplasty and stent placement (Alkashkari et al., 2019). Since the minimally invasive techniques result in faster recovery and they are cost-effective, they play a crucial role in treatment of CoA (Kwon et al., 2014). Stenting has the advantage of resisting re-coarctation better than balloon angioplasty (Kwon et al., 2014) and became popular to treat CoA. Whether the treatment is surgical or minimally invasive, coarctation repairs have a high rate of success in short term and mid-term (Alkashkari et al., 2019). A multi-center study showed that 98% of the coarctation repairs reduced the peak systolic pressure drop below 20 mmHg, which is the criteria for intervention (Forbes et al., 2007; Rao, 2020). Another study focused on stent placement and showed that it results in high survival rate and reduced pressure drop as well as increased diameter in the CoA region (Suárez de Lezo et al., 2015).

The results of CoA repair can also be simulated

Aslan, S., Liu, X., Wu, Q., Mass, P., Loke, Y., Hibino, N., Olivieri, L. and Krieger, A.
Virtual Planning and Simulation of Coarctation Repair in Hypoplastic Aortic Arches: Is Fixing the Coarctation Alone Enough?.
DOI: 10.5220/0010842600003123
In *Proceedings of the 15th International Joint Conference on Biomedical Engineering Systems and Technologies (BIOSTEC 2022) - Volume 3: BIOINFORMATICS*, pages 138-143
ISBN: 978-989-758-552-4; ISSN: 2184-4305

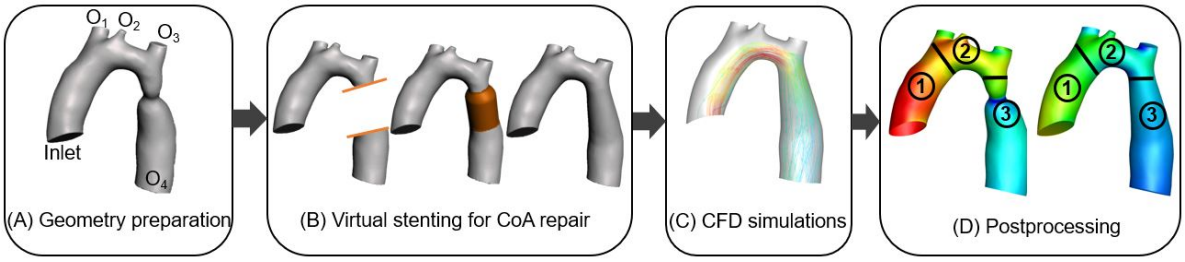

Figure 1: Schematic workflow of repairing CoA for patients with both CoA and TAH. (A) patient data acquisition and geometry preparation. (B) from left to right: separation of CoA region from the rest of the aorta, virtual stent placement, and final geometry after CoA repair. (C) performing CFD simulations. (D) postprocessing the results in the region of interest.

Table 1: Patients' demographics. BSA: body surface area (m^2), D_{CoA}: diameter of coarctation area, D_{Ao}: diameter of ascending aorta, D_{Arch}: diameter of aortic arch.

	BSA	Age	D_{CoA}/D_{Ao}	D_{Arch}/D_{Ao}
Case 1	1.27	9	0.43	0.67
Case 2	0.9	8	0.51	0.55
Case 3	0.38	9 mo	0.48	0.51

and analyzed using computational fluid dynamics (CFD) models. Combined with imaging, CFD can calculate not only pressure drop but also wall shear stress (WSS) which is the most studied flow parameter since the extremely high or low WSS is known to cause adverse effects on aorta walls (Dux-Santoy et al., 2020). CFD studies showed that WSS and peak systolic pressure drop (PSPD) were improved after CoA repair (Schubert et al., 2020; Goubergrits et al., 2015). However, even after a successful repair of coarctation, long-term complications may occur (Torok et al., 2015; Quennelle et al., 2015). Especially, an existing, untreated TAH can cause late systemic hypertension (Quennelle et al., 2015). Therefore, utilizing CFD to predict the outcomes of CoA repair in patients who also suffer from TAH may help clinicians to make decisions on treatment method.

In this study, we investigated whether the CoA repair with untreated TAH can provide satisfactory hemodynamic results. We identified three representative patient cases (n=3) with both CoA and TAH at different degrees. CoAs of the three patients were virtually treated using stents that were designed with commercially available stent dimensions. We performed CFD simulations to predict the pressure drop and TAWSS (time-averaged wall shear stress) of repaired aortas and analyzed the improvements. Our findings indicated that the efficacy of only repairing CoA varies in different patients. The results of this study showed that the hemodynamics predicted by CFD simulations in treatment planning stage may provide guidance for making clinical decision on whether to leave TAH untreated when repairing CoA.

2 METHODS

Figure 1 demonstrates the workflow that we followed in this study. The four steps include: (A) patient data acquisition and geometry preparation, (B) stent creation and virtual repairs of CoA, (C) CFD simulations of native and virtually repaired CoA geometries, and (D) postprocessing results. The details of each step were provided in the remainder of this section.

2.1 Patient Data Acquisition and Geometry Preparation

For this study, we selected three patients (n=3) who were diagnosed with CoA and TAH (based on the z-scores (Lopez et al., 2017)) with available Magnetic Resonance Imaging (MRI) data and non-invasive pressure measurements from arm and leg. The pulsatile flow rates in ascending and descending aortas were measured at the cross-sectional planes by 2-D phase-contrast cardiac magnetic resonance (CMR) imaging of each patient. The patients' demographics are provided in Table 1. We included the ratios of the diameters of the arch and CoA to ascending aorta (Ao) to provide the severity of TAH and CoA.

The data were acquired as part of and Institutional Review Board (IRB) approved retrospective study. Segmentation of images was performed using Mimics software (Materialise, Leuven, Belgium) to create three-dimensional (3-D) models of native aortas that included ascending aorta (inlet), brachiocephalic artery (O_1), left common carotid artery (O_2), left subclavian artery (O_3), and descending aorta (O_4), as shown in Figure 1A. The 3-D geometries then were smoothed to reduce rough surfaces of the models. The boundaries of the models were cut perpendicular to the flow direction and all boundaries were extruded 50 mm to avoid backflow in the simulations.

2.2 Stent Creation and Virtual Repair of Coarctation

The virtual stents were selected patient-specifically. Based on descending aorta size of each patient, a commercially available stent with appropriate length and diameter was chosen (Peters et al., 2009). The stent geometries were created using Solidworks (Waltham, MA, USA) software as circular cylinder to mimic the shape when it expands. Two cuts were made in the descending aorta of the patient to remove CoA region from the native geometry as shown in Figure 1B. Two planes that are parallel to and 2 mm away from the cut surfaces of the native tissue were created. A circle with the same diameter as the descending aorta was drawn on the distal plane and a straight solid extension was made to create the virtual stent. The stent was merged to distal and proximal sides of native tissue by lofting the surfaces. Lastly, the merged regions were smoothed using Autodesk Meshmixer software (San Rafael, CA, USA). The merged regions were selected separately and uniform triangles option was applied with a smoothing scale set to 50 and constraint rings set to 1. Additional robust smoothing was performed on the small rough surfaces by selecting them manually.

2.3 CFD Simulation

Tetrahedral meshes were generated for the native and virtually repaired models using ANSYS Mesh (Mesh, ANSYS, Canonsburg, PA, USA). The maximum and minimum sizes were chosen as 0.5 mm to have a uniform size of mesh elements since the results that are obtained using this size were previously validated (Aslan et al., 2020). An inflation layer with 5 layers, 1.2 growth rate, and 0.6 mm total thickness was created at the aorta walls to resolve the boundary layer. The number of total mesh elements of each model was at least 1 million. The governing flow equations that are given in (1) and (2), were solved using ANSYS Fluent assuming the blood is Newtonian (with a viscosity of 0.00371 Pa and density of 1060 kg/m^3) and the walls are rigid.

$$\frac{\partial \rho}{\partial t} + \nabla(\rho \overrightarrow{u}) = 0, \tag{1}$$

$$\rho \frac{D\overrightarrow{u}}{Dt} = -\nabla p + \rho \overrightarrow{g} + \nabla \tau_{ij} \tag{2}$$

In equations (1) and (2), ρ is density, u is velocity, τ is stress tensor, and t is time. The time step size for the computations was one fifth of the acquired flow time step size of CMR.

At the inlet of the ascending aorta, the acquired time-dependent velocity curve and at the outlets, Windkessel boundary conditions were specified. The Windkessel parameters were obtained, and patient-specific turbulent flow (k-epsilon model) simulations were performed following the steps in a previously validated study (Aslan et al., 2020). The simulations were run for 10 cardiac cycles. The converged results were used to obtain hemodynamics.

2.4 Postprocessing and Comparison of Hemodynamics

After obtaining CFD results, the hemodynamics was calculated in the entire aorta and three regions of the aorta: ① ascending, ② arch, and ③ descending as indicated in Figure 1D. The arch was defined as the region between the brachiocephalic artery and left subclavian artery. We reported TAWSS and PSPD, and comparison between the native and virtually repaired CoA models.

3 RESULTS

The pressure distribution for each case before and after virtual CoA repair are shown in Figure 2. The repair of CoA reduced the maximum pressure in the ascending aorta for all cases. In the descending part, the pressure is more uniformly distributed after the virtual treatment. The PSPD across the entire aorta of each patient were obtained and listed in Table 2.

The virtual CoA repair decreased the PSPD for Case 1 and Case 3 by 9.3 mmHg and 9.57 mmHg, respectively. However, Case 2 did not show significant improvement after the repair. From a clinical perspective, 20 mmHg pressure difference is an indicator of intervention or reintervention to repair aortic disease. The CoA repair successfully decreased PSPD below 20 mmHg in Case 1. Although the PSPD of Case 3 was reduced by 24% after the virtual repair, the pressure difference remained higher than 20 mmHg. For Case 2, the PSPD was close to the 20 mmHg limit be-

Table 2: The comparison of PSPD between native and repaired CoA geometries for three cases.

		PSPD (mmHg)
Case 1	Native	24.72
	Repaired CoA	15.42
Case 2	Native	17.45
	Repaired CoA	17.26
Case 3	Native	44.27
	Repaired CoA	34.70

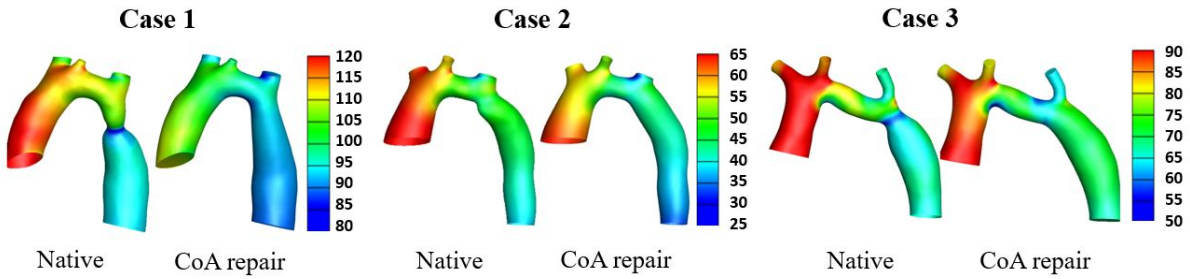

Figure 2: The pressure distribution of native and repaired CoA models of three cases. The unit of the pressure scale is mmHg.

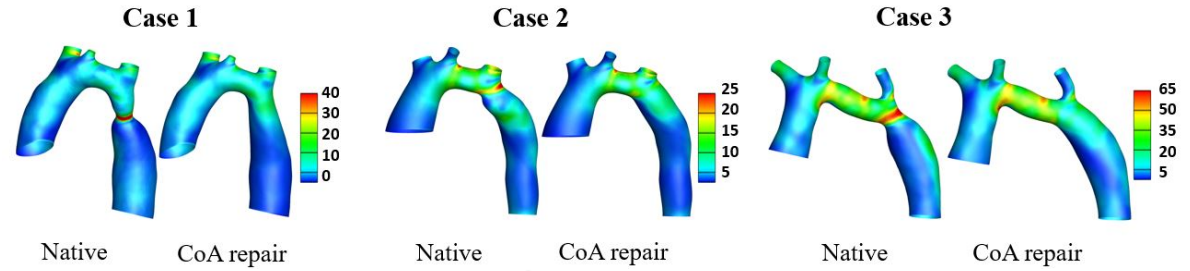

Figure 3: The TAWSS distribution of native and repaired CoA models of three cases. The unit of the TAWSS scale is Pascal (Pa).

fore the virtual repair and it remained the same post-repair.

The PSPD were calculated in region ② (arch) and ③ (descending) of the aorta to identify the contribution of TAH to the overall PSPD after the CoA repair. The results are shown in Table 3. The CoA repair decreased the PSPD in region ③ by 12 mmHg and 1 mmHg for Case 1 and 3, respectively. The PSPDs in region ② after the repair were 7.9 mmHg for Case 1, 24.1 mmHg for Case 3. TAH contributed more to the overall PSPD than CoA. For Case 2, the changes after the CoA repair were similar with higher PSPD in region ② than region ③.

Compared to Case 1 and 3, the descending aorta of Case 2 was the longest (61% of overall aorta length) and the percent increase in diameter after the CoA repair was the smallest (22%). Therefore, a larger PSPD in descending part and a smaller change in overall PSPD after the CoA repair for Case 2 is expected.

The TAWSS distributions for the three patients are shown in Figure 3. The highest magnitudes of

Table 3: The comparison of PSPD in TAH region ② and CoA region ③ after CoA repair.

	Region	PSPD (mmHg)
Case 1	②	7.9
	③	1.0
Case 2	②	7.3
	③	5.6
Case 3	②	24.1
	③	2.0

Table 4: The comparison of maximum TAWSS between native and repaired CoA geometries for the three patients.

	Geometry	TAWSS (Pa)
Case 1	Native	38
	Repaired CoA	18
Case 2	Native	26
	Repaired CoA	16
Case 3	Native	70
	Repaired CoA	34

TAWSS were observed in Case 3. The virtual stent repair fixed the region with high TAWSS in the CoA area and all three cases showed reduced maximum TAWSS after the repair. The maximum TAWSS values in the descending aorta before and after the repair are shown in Table 4. The improvement in TAWSS was in the repaired region but the magnitudes remained higher than the rest of the overall TAWSS in descending aorta for all cases. The TAWSS in the aortic arch of Case 3 was high in the native case and since the TAH in the arch was not repaired, the TAWSS remained the same in that region. The higher values of TAWSS in the arch and repaired CoA region persisted even after the CoA repair compared to the rest of the aorta but overall magnitudes of TAWSS in the descending aorta decreased compared to the native cases.

4 DISCUSSION

This study focused on evaluating PSPD and TAWSS of three patients with conditions of TAH and CoA. We investigated the improvements in hemodynamics after repairing only CoA virtually via stent placement and leaving TAH untreated. Although the same virtual treatment was applied to all three patients who were diagnosed with the same diseases, the improvement in PSPD after the CoA repair was inconsistent. One of the cases showed almost no reduction in PSPD and one other case showed 9 mmHg reduction with the PSPD still higher than 20 mmHg, the typical threshold for intervention. Only one case successfully decreased PSPD from a higher value to below 20 mmHg. The pressure drops in TAH regions contributed more to overall PSPD than pressure drops in descending aorta. The results suggest that the CoA repair alone in patients who also suffer from TAH does not guarantee satisfactory PSPD in all cases. It should be noted that the case with the PSPD higher than 20 mmHg after the repair was the youngest patient case, a 9 months old infant. In very young patient cases, the doctors would opt for surgical repair of isolated coarctations, thus the virtual stenting may not necessarily apply for Case 3 which may have influenced the results.

A TAWSS that is higher than 50 dyne/cm^2 (5 Pa) is shown to be associated with platelet aggregation in previous studies (Kwon et al., 2014). The higher values of WSS were observed in descending aorta even after CoA repair. But the region with the high TAWSS was the proximal region where descending aorta and left subclavian artery connects and it is a very small area compared to the entire descending aorta region. The TAWSS in the aortic arch was very high compared to repaired CoA region, especially for Case 3, reaching up to 60 Pa. Therefore, platelet formation could likely occur in this region due to untreated TAH.

The limitations of this study include the rigid assumption of the aorta walls to simplify the computation and reduce the computation time. Since the assumption was made for all models and the purpose of this study was to demonstrate improvements in hemodynamics compared to native geometries, the rigid wall assumption does not significantly affect the comparison. Also, previous studies (Siogkas et al., 2011) showed that the results of the blood flow simulations obtained in arterial segments assuming rigid walls and modeling deformable walls were similar. Although the number of patient cases is small to draw a conclusion for answering the question proposed in the title, we demonstrated a systematic method for virtual planning and simulation of CoA repair that can be used for more cases. In addition, the anatomy of each aorta was distinctive which allowed observing different improvements in results after virtual CoA repair.

The method we used in this study to predict the PSPD was previously validated in cases with CoA by comparing the simulation results and invasive pressure measurements from the patients (Aslan et al., 2020). We performed virtual repair of CoA to investigate the changes in PSPD. In a future study, invasive PSPD measurements of the patients after the stent placement could be used to validate the simulation results of virtual CoA repairs.

Lastly, we modeled different size stents based on patient-specific length and diameters and used one type of repair to increase CoA diameter. In clinical applications, different type of stents may result in different hemodynamics, affecting the TAWSS in particular (Kwon et al., 2014) in the repaired CoA region. Therefore, it may affect the virtual treatment planning for CoA repair and should be taken into consideration.

This study used virtual repair and CFD to help doctors determine whether the CoA treatment alone is sufficient in patients who also suffer from TAH. In a future study, virtual treatment could be performed to repair both CoA and TAH to help clinicians decide if replacing minimally invasive stent treatment with a surgery to repair both defects in different patients would be more advantageous.

5 CONCLUSIONS

We investigated the improvements in PSPD and TAWSS after repairing the CoA using virtual stents in aortas that also have TAH. We showed that after repairing the CoA, TAWSS was improved in the descending aorta and PSPD was not always satisfactory. Patient-specific stent selection, stent placement, and flow simulations were performed. This study is the first to investigate whether the stent repair that caries less risks for patients than a surgery would result in satisfactory PSPD and TAWSS in patient who also suffers from TAH. The results of our study could help clinicians determine the most appropriate treatment in patients with CoA and TAH. Combination of imaging and patient-specific CFD simulations is an important tool in treatment planning and could change the selection and outcomes of repairs.

ACKNOWLEDGEMENTS

This work was supported by National Institute of Health under grants NHLBI-R01HL143468 and R21/R33HD090671. The authors acknowledge the

supercomputing resource at the Advanced Research Computing at Hopkins (ARCH) that made available for conducting the research reported in this paper.

REFERENCES

Alkashkari, W., Albugami, S., and Hijazi, Z. M. (2019). Management of coarctation of the aorta in adult patients: state of the art. *Korean circulation journal*, 49(4):298–313.

Aslan, S., Mass, P., Loke, Y.-H., Warburton, L., Liu, X., Hibino, N., Olivieri, L., and Krieger, A. (2020). Non-invasive prediction of peak systolic pressure drop across coarctation of aorta using computational fluid dynamics. In *2020 42nd Annual International Conference of the IEEE Engineering in Medicine & Biology Society (EMBC)*, pages 2295–2298.

Dux-Santoy, L., Guala, A., Sotelo, J., Uribe, S., Teixidó-Turà, G., Ruiz-Muñoz, A., Hurtado, D. E., Valente, F., Galian-Gay, L., Gutiérrez, L., et al. (2020). Low and oscillatory wall shear stress is not related to aortic dilation in patients with bicuspid aortic valve: a time-resolved 3-dimensional phase-contrast magnetic resonance imaging study. *Arteriosclerosis, thrombosis, and vascular biology*, 40(1):e10–e20.

Forbes, T. J., Garekar, S., Amin, Z., Zahn, E. M., Nykanen, D., Moore, P., Qureshi, S. A., Cheatham, J. P., Ebeid, M. R., Hijazi, Z. M., et al. (2007). Procedural results and acute complications in stenting native and recurrent coarctation of the aorta in patients over 4 years of age: a multi-institutional study. *Catheterization and Cardiovascular Interventions*, 70(2):276–285.

Goubergrits, L., Riesenkampff, E., Yevtushenko, P., Schaller, J., Kertzscher, U., Berger, F., and Kuehne, T. (2015). Is mri-based cfd able to improve clinical treatment of coarctations of aorta? *Annals of biomedical engineering*, 43(1):168–176.

Kenny, D., Polson, J. W., Martin, R. P., Paton, J. F., and Wolf, A. R. (2011). Hypertension and coarctation of the aorta: an inevitable consequence of developmental pathophysiology. *Hypertension Research*, 34(5):543–547.

Kwon, S., Feinstein, J. A., Dholakia, R. J., and LaDisa, J. F. (2014). Quantification of local hemodynamic alterations caused by virtual implantation of three commercially available stents for the treatment of aortic coarctation. *Pediatric cardiology*, 35(4):732–740.

Liu, X., Aslan, S., Hess, R., Mass, P., Olivieri, L., Loke, Y., Hibino, N., Fuge, M., and Krieger, A. (2020). Automatic shape optimization of patient-specific tissue engineered vascular grafts for aortic coarctation. In *2020 42nd Annual International Conference of the IEEE Engineering in Medicine & Biology Society (EMBC)*, pages 2319–2323.

Lopez, L., Colan, S., Stylianou, M., Granger, S., Trachtenberg, F., Frommelt, P., Pearson, G., Camarda, J., Cnota, J., Cohen, M., et al. (2017). Relationship of echocardiographic z scores adjusted for body surface area to age, sex, race, and ethnicity: the pediatric heart network normal echocardiogram database. *Circulation: Cardiovascular Imaging*, 10(11):e006979.

Ma, Z.-L., Yan, J., Li, S.-J., Hua, Z.-D., Yan, F.-X., Wang, X., and Wang, Q. (2017). Coarctation of the aorta with aortic arch hypoplasia: midterm outcomes of aortic arch reconstruction with autologous pulmonary artery patch. *Chinese medical journal*, 130(23):2802.

Mai, C. T., Isenburg, J. L., Canfield, M. A., Meyer, R. E., Correa, A., Alverson, C. J., Lupo, P. J., Riehle-Colarusso, T., Cho, S. J., Aggarwal, D., et al. (2019). National population-based estimates for major birth defects, 2010–2014. *Birth defects research*, 111(18):1420–1435.

Peters, B., Ewert, P., and Berger, F. (2009). The role of stents in the treatment of congenital heart disease: Current status and future perspectives. *Annals of pediatric cardiology*, 2(1):3.

Quennelle, S., Powell, A. J., Geva, T., and Prakash, A. (2015). Persistent aortic arch hypoplasia after coarctation treatment is associated with late systemic hypertension. *Journal of the American Heart Association*, 4(7):e001978.

Rao, P. S. (2020). Neonatal (and infant) coarctation of the aorta: management challenges. *Research and Reports in Neonatology*, 10:11.

Schubert, C., Brüning, J., Goubergrits, L., Hennemuth, A., Berger, F., Kühne, T., and Kelm, M. (2020). Assessment of hemodynamic responses to exercise in aortic coarctation using mri-ergometry in combination with computational fluid dynamics. *Scientific Reports*, 10(1):1–12.

Siewers, R. D., Ettedgui, J., Pahl, E., Tallman, T., and Pedro, J. (1991). Coarctation and hypoplasia of the aortic arch: will the arch grow? *The Annals of thoracic surgery*, 52(3):608–613.

Siogkas, P., Sakellarios, A., Exarchos, T., Stefanou, K., Fotiadis, D., Naka, K., Michalis, L., Filipovic, N., and Parodi, O. (2011). Blood flow in arterial segments: rigid vs. deformable walls simulations. *Journal of the Serbian Society for Computational Mechanics*, 5(1):69–77.

Suárez de Lezo, J., Romero, M., Pan, M., Suárez de Lezo, J., Segura, J., Ojeda, S., Pavlovic, D., Mazuelos, F., López Aguilera, J., and Espejo Perez, S. (2015). Stent repair for complex coarctation of aorta. *Cardiovascular Interventions*, 8(10):1368–1379.

Torok, R. D., Campbell, M. J., Fleming, G. A., and Hill, K. D. (2015). Coarctation of the aorta: management from infancy to adulthood. *World journal of cardiology*, 7(11):765.